Ab initio calculation of d–d excitations in quasi-one-dimensional Cu d^9 correlated materials

Hsiao-Yu Huang,[1, 2, 3] Nikolay A. Bogdanov,[1, 4] Liudmila Siurakshina,[1, 5, 6]
Peter Fulde,[5, 7] Jeroen van den Brink,[1] and Liviu Hozoi[1]

[1] *Institute for Theoretical Solid State Physics, IFW Dresden, Helmholtzstr. 20, 01069 Dresden, Germany*
[2] *College of Science, National Tsing Hua University, 30013 Hsinchu, Taiwan*
[3] *National Synchrotron Radiation Research Center, Hsin-Ann Rd. 101, 30076 Hsinchu, Taiwan*
[4] *National University of Science and Technology MISIS, Leninskiy pr. 4, 119049 Moscow, Russia*
[5] *Max-Planck-Institut für Physik komplexer Systeme, Nöthnitzer Str. 38, 01187 Dresden, Germany*
[6] *Laboratory of Information Technologies, Joint Institute for Nuclear Research, 141980 Dubna, Russia*
[7] *POSTECH, San 31 Hyoja-dong, Namgu Pohang, Gyeongbuk 790-784, Korea*
(Dated: February 18, 2022)

With wavefunction-based electronic-structure calculations we determine the Cu d–d excitation energies in quasi-one-dimensional spin-chain and ladder copper oxides. A complete set of local excitations has been calculated for cuprates with corner-sharing (Sr_2CuO_3 and $SrCuO_2$) and edge-sharing ($LiVCuO_4$, $CuGeO_3$, $LiCu_2O_2$ and Li_2CuO_2) CuO_4 plaquettes, with corner-sharing CuF_6 octahedra ($KCuF_3$), for the ladder system $CaCu_2O_3$, and for multiferroic cupric oxide CuO. Our data compare well with available results of optical absorption measurements on $KCuF_3$ and the excitation energies found by resonant inelastic x-ray scattering experiments for CuO. The *ab initio* results we report for the other materials should be helpful for the interpretation of future resonant inelastic x-ray scattering experiments on those highly anisotropic compounds.

I. INTRODUCTION

Many-body effects within the partially filled $3d$ shells of transition-metal oxides are at the heart of various intriguing phenomena. Much of the interesting physics comes from the interplay between electron delocalization caused by intersite orbital overlap and strong Coulomb interactions within the d shell. The investigation of this interplay goes back as far as the 1930's with the work of Verwey, Mott, and others.[1] Additional degrees of freedom arising from orbital degeneracy, electron-lattice couplings, and/or ligand p to metal d charge transfer effects increase in many cases the complexity of the problem. Further, it was found that the multiorbital couplings within the $3d$ shell may be strong even when the orbital degeneracy is lifted, e.g., by the electrostatic field set up by neighboring ions. For the copper oxide superconductors, for example, it is believed that the off-diagonal coupling between states of x^2–y^2 and z^2 symmetry is one of the elements which determine the precise shape of the Fermi surface, see, e.g., 2–6 and references therein. Accurate estimates for the size of the d-level splittings are therefore important in designing realistic model Hamiltonians for these systems.

Traditionally the d–d excitations in transition-metal oxides have been investigated by optical spectroscopy. First measurements on rocksalt compounds such as NiO and CoO were reported in the late 50's.[7] Although in centro-symmetric cases these transitions are not dipole allowed, they do aquire weak intensity in the optical spectra due to the admixture of lattice vibrations which lift the inversion symmetry at the transition-metal site.

It has been shown recently that highly accurate measurements for both magnetic and local charge excitations can be carried out by resonant inelastic x-ray scattering (RIXS).[8] As demonstrated by Moretti Sala *et al.*[9] for the case of d–d transitions in two-dimensional (2D) Cu oxide systems, the high energy resolution and the analysis of the polarization and scattering geometry dependence allow a quite reliable interpretation as concerns the nature of the final excited states.

The calculation of local excitations within the transition-metal $3d$ shell is an interesting problem. It is desirable to use alternative approaches to standard density functional theory (DFT) calculations because in first place electron correlations are strong and secondly, in its original formulation, DFT is only a ground-state theory. The *ab initio* wavefunction-based quantum chemical approaches therefore constitute the method of choice here. Advanced quantum chemical calculations have been recently applied to the study of d–d excitations in La_2CuO_4, $Sr_2CuO_2Cl_2$, and $CaCuO_2$. The *ab initio* results[10] turned out to be in good agreement with the RIXS data reported by Moretti Sala *et al.*[9] On the other hand, recent DFT calculations on La_2CuO_4 predict $d_{x^2-y^2}$ to d_{z^2} excitation energies that are 0.5 eV lower than in experiment.[6,9]

Here, we extend the study of 2D cuprates as in Ref. 10 to the case of highly anisotropic chain and ladder Cu d^9 compounds. The motivation for the present investigation is twofold. One one hand, we want to check the performance of our quantum chemical computational scheme[10] in the case of one-dimensional (1D) and quasi-1D Cu d^9 systems. Quantum chemical calculations on relatively small clusters have been earlier performed on both 2D and 1D cuprates, e.g., the 2D layered materials La_2CuO_4 and $Sr_2CuO_2Cl_2$ and the chain-like system Sr_2CuO_3.[11] However, differences as large as 0.5 eV were found between the on-site d–d excitation energies reported for

La$_2$CuO$_4$ and Sr$_2$CuO$_2$Cl$_2$ in Ref. 11 and our more recent results discussed in Ref. 10. Those differences seem to be related to the less precise description in Ref. 11 of the adjacent 3d-metal and O ions, i.e., the nearest neighbor (NN) Cu ions and ligands around the CuO$_4$ plaquette at which the d–d excited states are explicitly computed. Similar differences are here found for the d-level splittings of the chain system Sr$_2$CuO$_3$, which shows that a careful analysis of this issue is indeed motivated.

Secondly, our *ab initio* data should be helpful for the correct interpretation of RIXS and optical spectra in these compounds. For highly anisotropic structures, the degeneracy of both the t_{2g} and e_g levels is lifted and the excitation spectra display a very rich structure. Even in the 2D compounds, the sequence of the different excited states cannot always be predicted beforehand. For example, due to the different ratios between the in-plane and apical Cu–O bond lengths, the z^2 hole state corresponds to the lowest crystal-field excited state in La$_2$CuO$_4$, with a relative energy of 1.4 eV,[9,10] and to the highest crystal-field excitation in HgBa$_2$CuO$_4$, with a relative energy of 2.1 eV.[10] The situation should be even more complex in 1D systems. Reliable *ab initio* results are therefore desirable for the chain and ladder cuprates.

II. COMPUTATIONAL DETAILS

Our computational approach is based on correlated *ab initio* methods traditionally used in quantum chemical studies on molecular systems. For each of the materials investigated here, the starting point is a restricted Hartree-Fock (RHF) calculation with periodic boundary conditions. All RHF calculations were performed with the CRYSTAL program package.[12] We applied Gaussian-type atomic basis sets from the CRYSTAL library, i.e., basis functions of triple-zeta quality[26] for Cu, O, and F and basis sets of either double-zeta or triple-zeta quality for metal ions next to the CuO$_2$ chains (e.g., Li, Ca or V). In all computations experimental lattice parameters were used, as reported in Refs. 13–21.

Post Hartree-Fock correlation calculations can be carried out on finite embedded clusters, due to the local character of the correlation hole of a d electron. Yet, the orbitals used here are those of the infinite system. Each embedded cluster $\mathcal{C}$ consists of two distinct regions: an active region $\mathcal{C}_A$ where the actual correlation treatment is performed and a buffer region $\mathcal{C}_B$ whose role is to provide support for the longer-range tails of Wannier orbitals (WO's) centered at sites in $\mathcal{C}_A$. The active region $\mathcal{C}_A$ includes one reference Cu site, the NN ligands, and the NN Cu ions. For the systems addressed in this study, a given Cu ion may have four, five or six NN ligands. Those NN ligands thus form either L$_4$ plaquettes, L$_5$ pyramids or distorted L$_6$ octahedra around a particular Cu site. As concerns the $\mathcal{C}_B$ region, we include in there each ligand coordination cage around the NN Cu sites and all NN closed-shell metal ions. In CuGeO$_3$, for example, there

are 8 Ge^{4+} NN's. In LiCu$_2$O$_2$, there are 5 Cu^{1+} 3d^{10} and 8 Li^{1+} NN's. All post-RHF computations were performed with the MOLPRO quantum chemical software.[22]

The orbital basis associated with a given cluster $\mathcal{C}$ is a set of projected WO's: localized WO's associated with the RHF bands are first derived with the help of the orbital localization module of the CRYSTAL package and subsequently projected onto the set of Gaussian basis functions associated with the atomic sites within the cluster $\mathcal{C}$. Technicalities concerning this procedure are discussed in Refs. 10, 23, and 24. For each particular cluster, the RHF data is additionally used to generate an one-electron embedding potential that models the crystalline environment. This effective potential is constructed with the MATROP module of the MOLPRO program by using a real-space matrix representation of the self-consistent Fock operator from the periodic RHF calculation.[23,24] All necessary RHF data is converted into MOLPRO format with the help of an interface program.[25] Although the WO's at the atomic sites of $\mathcal{C}$ are derived for each of the compounds discussed here by periodic RHF calculations for the Cu 3d^9 electron configuration, the embedding potentials are obtained by replacing the Cu^{2+} 3d^9 ions by closed-shell Zn^{2+} 3d^{10} species. This is a good approximation for the farther 3d-metal sites, as the comparison between our results and RIXS data shows.[9,10] The extension of this embedding scheme toward the construction of open-shell embeddings is an ongoing project in our group.

While the occupied WO's in the buffer region $\mathcal{C}_B$ are kept frozen, all valence orbitals centered at ligand and Cu sites in $\mathcal{C}_A$ are further reoptimized[10] in multiconfiguration complete-active-space self-consistent-field (CASSCF) calculations.[26] In the latter, the ground-state wavefunction and the crystal-field excited states at the central Cu site are computed by state-averaged multiroot optimizations.[26] The Cu d-level splittings are finally obtained from additional multireference single and double configuration-interaction[26] (MRCI) calculations as the relative energies of the crystal-field excited states. The central Cu 3s, 3p, 3d, NN ligand 2p, and NN half-filled Cu 3d orbitals are correlated in MRCI.

The virtual orbital space in the MRCI calculation cannot be presently restricted just to the $\mathcal{C}_A$ region. It thus includes virtual orbitals in both $\mathcal{C}_A$ and $\mathcal{C}_B$, which leads to very large MRCI expansions. To make the computations feasible, we restrict our study to ferromagnetic (FM) allignment of the Cu d spins. Even for FM clusters, the MRCI expansion may include in some cases up to $\sim 10^{11}$ Slater determinants.

III. RESULTS AND DISCUSSIONS

A. Chains of corner-sharing CuO$_4$ plaquettes

The 1D compounds Sr$_2$CuO$_3$ and SrCuO$_2$, built of chains of corner-sharing CuO$_4$ plaquettes, display a

number of quite unusual properties. On one hand, these materials have the largest NN antiferromagnetic (AF) exchange integrals in the family of Cu d^9 oxides. Yet, the interchain couplings are very weak.[27–32] They thus constitute ideal systems for studying the magnetic response of 1D spin-1/2 antiferromagnets. Secondly, high-resolution angle-resolved photoemission experiments on these compounds have for the first time revealed the realization of spin-charge separation in 1D electron systems.[33,34]

We list in Table I results for the d-level splittings of Sr_2CuO_3 and $SrCuO_2$. As concerns the crystallographic details, a major difference between these two compounds is the presence of a network of single CuO_2 chains in Sr_2CuO_3,[13] see Fig. 1, whereas $SrCuO_2$ displays a double-chain structure, with CuO_4 plaquettes on adjacent chains sharing common edges.[14] The clusters we use in our CASSCF and MRCI calculations include therefore two NN plaquettes in the case of Sr_2CuO_3 and four adjacent plaquettes for $SrCuO_2$. The reference system is chosen such that the x-axis is along the CuO_2 chains and z is perpendicular onto the CuO_4 plaquettes. In this framework, the ground-state hole orbital has x^2-y^2 symmetry. The data in Table I show that the d-level splittings in Sr_2CuO_3 and $SrCuO_2$ are very similar. In both cases, the relative energy of each particular excited state is not very different from the corresponding value in the Li_2CuO_2 compound, see Sec. III.C. As in Sr_2CuO_3 and $SrCuO_2$, there are no apical ligands in Li_2CuO_2 either. Results for the d-level electronic structure of the latter compound are listed in Table III.

Inclusion of single and double excitations on top of the CASSCF wavefunctions brings a nearly uniform upward shift of 0.1 to 0.2 eV for the d–d transitions. By adding Davidson corrections,[35] the relative energies of the excited states further increase by 0.05 to 0.1 eV. The MRCI values listed in Table III include such Davidson correction terms. This relative stabilization of the electronic ground state with respect to the higher lying states in MRCI is mainly related to ligand $2p$ to metal $3d$ charge-
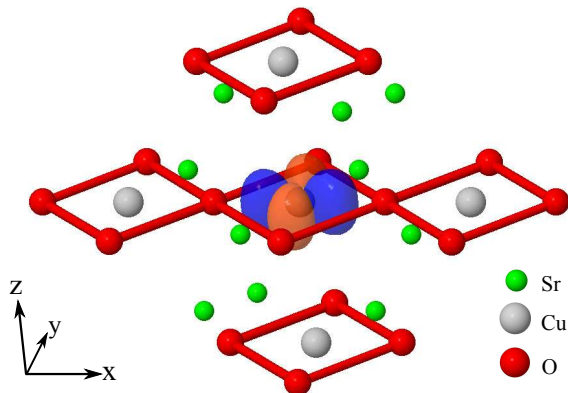

FIG. 1. Chain of corner-sharing CuO_4 plaquettes in Sr_2CuO_3. The ground-state hole orbital is $d_{x^2-y^2}$.

TABLE I. CASSCF/MRCI d–d excitation energies for corner-sharing chains of CuO_4 plaquettes in Sr_2CuO_3 and $SrCuO_2$ (eV). The MRCI values include Davidson corrections.[35]

Hole orbital	Sr_2CuO_3 CASSCF/MRCI	$SrCuO_2$ CASSCF/MRCI
x^2-y^2	0	0
xy	1.20/1.50	1.26/1.55
yz	1.83/2.14	1.77/2.03
xz	1.90/2.24	1.88/2.19
z^2	2.16/2.55	2.08/2.44

transfer correlation effects which are more important for the in-plane $d_{x^2-y^2}$ hole orbital having σ-type overlap with the NN O $2p$ functions.

As concerns the comparison with other theoretical investigations, there are differences of 0.3 eV or more between the d–d excitation energies listed for Sr_2CuO_3 in Table I and the values computed earlier in Ref. 11. We presume that these large differences, e.g., about 0.5 eV for the yz hole states, are mainly related to the approximations used in Ref. 11 for representing the Cu and O ions on NN plaquettes. While here we represent those species at the all-electron level, in the earlier study[11] the NN Cu and O ions were modeled by Mg^{2+} ions and formal $2-$ point charges, respectively. Point charges were also used for the embedding in Ref. 11.

We note at this point that in an AF lattice the total energy of a given state within the d^n manifold is a sum of a crystal-field contribution, i.e., an on-site crystal-field splitting, and a magnetic term (see also the discussion in Refs. 8 and 10). As mentioned above, the AF NN spin coupling constant J is remarkably large in Sr_2CuO_3 and $SrCuO_2$, 0.20 to 0.25 eV[27–31]. From the exact Bethe-ansatz solution for the 1D Heisenberg Hamiltonian,[36–38] the AF ground-state stabilization energy is $J \ln 2$. On the other hand, from overlap considerations, we conclude that for the crystal-field excited states the (super)exchange with the NN Cu $d_{x^2-y^2}$ spins is either zero or much weaker. For technical reasons, see the discussion in Sec. II, the quantum chemical calculations were here performed for a FM cluster. For a meaningful comparison between the MRCI results and experimental RIXS data, one should therefore subtract a term $J \ln 2$ from the relative RIXS energies, representing the energy stabilization of the AF ground-state with respect to the crystal-field excited states. These considerations are relevant in light of future RIXS measurements on AF 1D cuprates.

B. Corner-sharing CuF_6 octahedra in $KCuF_3$

$KCuF_3$ is a prototype material for systems with strong coupling among the charge, orbital, and spin degrees of freedom.[39,40] The crystalline structure of this compound is perovskite-like,[15] i.e., three-dimensional (3D). The de-

TABLE II. Cu d–d excitation energies in KCuF$_3$ (eV). The ground-state Cu $t_{2g}^6 d_{y^2}^2 d_{x^2-z^2}^1$ configuration is taken as reference. The Jahn-Teller distortions occur within the xy plane. The MRCI values include Davidson corrections.[35]

Hole orbital	CASSCF	MRCI	Experiment[a]
$x^2 - z^2$	0	0	0
y^2	0.76	0.85	$0.71 - 1.02$
xz	0.89	1.01	$1.05 - 1.15$
xy	1.04	1.17	$1.21 - 1.37$
yz	1.11	1.25	$1.34 - 1.46$

[a]: Optical absorption, Ref. 43. The numbers correspond to the onsets and the maxima of the absorption bands.

generacy of the Cu e_g levels in an ideal perovskite lattice is lifted however through cooperative Jahn-Teller distortions. The latter imply a configuration with alternating, longer and shorter, Cu–F bonds for Cu ions along the x and y axes and orbital ordering in the xy plane. The hole in the Cu $3d$ shell thus alternately occupies $3d_{x^2-z^2}$ and $3d_{y^2-z^2}$ orbitals.

In the xy plane, the magnetic couplings are weak and FM. On the other hand, along the z-axis the NN J is large and AF.[41] Actually this makes KCuF$_3$ a close to ideal 1D Heisenberg antiferromagnet. The predictions for the low-lying spin excitations of the 1D AF Heisenberg chain[37,38] have been confirmed by inelastic neutron scattering experiments.[42]

The magnetic behavior changes from 1D to 3D at the Néel temperature $T_N = 39$ K. The emergence of sharp crystal-field absorption peaks in the optical spectra approximately 10 K above T_N has been interpreted as evidence for a symmetry change related with a crossover from dynamic to static displacements of the F ions.[43] In this picture, the orbital and 3D AF ordering are intimately related, in the sense that the former paves the road for the latter.

The d–d excitation energies seen in the optical spectra were compared in Ref. 43 with the outcome of DFT band-structure calculations. However, strictly speaking, DFT is a ground-state theory. Here, we provide results of excited-state CASSCF and MRCI calculations for the Cu d-level splittings in KCuF$_3$, see Table V. The MRCI treatment brings corrections of 0.1–0.15 eV to the CASSCF splittings, somewhat smaller than for the oxides discussed above. This is related to the more ionic character of the Cu–F bond in KCuF$_3$ and smaller degree of Cu $3d$ and F $2p$ orbital mixing. As a general trend, the MRCI results tend to slightly underestimate the values corresponding to the maxima of the experimental absorption peaks, by 0.1–0.2 eV. One obvious effect of the less anisotropic environment is a much smaller splitting between the two e_g components. This particular electronic-structure parameter is in fact the smallest among the Cu d^9 compounds investigated here.

C. Chains of edge-sharing CuO$_4$ plaquettes

Cuprates in which the CuO$_4$ plaquettes are edge-sharing, are characterized by weak superexchange interactions between NN Cu spins, which is due to Cu–O–Cu bond angles that are close to perpendicular. Depending on the detailed crystal structure, the NN interaction is usually FM (LiVCuO$_4$, Li$_2$CuO$_2$)[44–46] or even AF (CuGeO$_3$).[47,48] The in-chain next-NN exchange is always AF and causes frustration independently of the sign and size of the NN coupling. Further, the longer-range intrachain and interchain couplings are sizeable as well in some of these compounds and lead to an intricate competition of magnetic interactions. This has resulted in an appreciable scientific interest in the edge-sharing chain systems.

In LiVCuO$_4$ the ratio of the FM NN coupling and the AF next-NN exchange – the frustration parameter – is controversial.[44,45] For LiCu$_2$O$_2$ even the sign of the NN coupling constant gave rise to debate.[49–51] It has been also argued that a large fourth-nearest-neighbor AF coupling constant is responsible for the incommensurate helimagnetic ground state of LiCu$_2$O$_2$.[49] In CuGeO$_3$ the NN exchange is AF and this system is famous to undergo a so-called spin-Peierls transition[47,48] to an AF state with a gapped excitation spectrum. When deriving the values of the shorter- and longer-range exchange interactions in terms of downfolding techniques, also the $3d$-level excitation energies come into play.

The calculated CASSCF and MRCI results for the Cu d-level splittings in LiVCuO$_4$, CuGeO$_3$, LiCu$_2$O$_2$, and Li$_2$CuO$_2$ are listed in Table III. The finite embedded clusters on which the correlation treatment is carried out include one central and two NN CuO$_4$ plaquettes for the single chain compounds LiVCuO$_4$, CuGeO$_3$, and Li$_2$CuO$_2$. For the zigzag double-chain system LiCu$_2$O$_2$,[19] the cluster $\mathcal{C}$ includes four adjacent plaquettes. The coordinate framework is chosen such that the
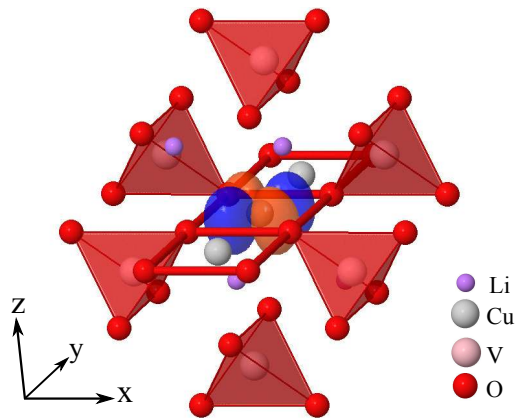

FIG. 2. Chain of edge-sharing CuO$_4$ plaquettes in LiVCuO$_4$. The ground-state hole orbital is d_{xy} in the chosen reference system. The six NN VO$_4$ octahedra around the reference Cu site are highlighted in the figure.

TABLE III. CASSCF/MRCI d–d excitation energies for edge-sharing chains of CuO_4 plaquettes (eV). The MRCI values include Davidson corrections.[35] The y-axis is parallel to the CuO_2 chains, z is perpendicular onto the CuO_4 plaquettes, see text.

Hole orbital	LiVCuO$_4$	CuGeO$_3$	LiCu$_2$O$_2$	Li$_2$CuO$_2$
xy	0	0	0	0
$x^2 - y^2$	1.08/1.28	1.19/1.41	1.13/1.43	1.20/1.52
xz	1.25/1.47	1.42/1.61	1.58/1.88	1.72/2.04
yz	1.29/1.52	1.45/1.64	1.64/1.94	1.72/2.04
z^2	0.98/1.18	1.50/1.71	1.67/1.98	1.93/2.30

y-axis is parallel to the CuO_2 chains and z is perpendicular onto a given CuO_4 plaquette. In other words, there is a rotation of $45°$ around z as compared to the standard coordinate framework for planar or octahedral coordination and the x and y axes are not along the in-plane Cu–O bonds. The in-plane σ-type Cu $3d$ orbital that is singly occupied in the ground-state configuration is thus denoted d_{xy}.

As for the corner-sharing plaquettes in Sr_2CuO_3 and $SrCuO_2$ (see Sec. III.A), inclusion of single and double excitations on top of the CASSCF wavefunctions brings a nearly uniform upward shift of 0.1 to 0.2 eV for the d–d transitions. By adding Davidson corrections, the relative energies of the excited states further increase by 0.05 to 0.1 eV. The MRCI values listed in Table III include such Davidson correction terms. A second effect which deserves attention is the large variations found for the relative energy of the d_{z^2} excited hole state. It is known that the length of the apical Cu–O bond varies widely in Cu d^9 oxides. The strong influence of the apical bond length on the d_{z^2} hole excitation was previously stressed for 2D cuprates in, e.g., Refs. 9 and 10. Using simple electrostatic arguments, when the negative apical ions are closer to the Cu site, less energy is required for exciting the in-plane Cu $3d$ hole to the d_{z^2} orbital pointing toward those apical ligands. As concerns the chain-like compounds from Table III, there are two apical O ions in $CuGeO_3$, one apical in $LiCu_2O_2$, and no apical ligand in Li_2CuO_2. The relative energy of the d_{z^2} hole state consequently increases from 1.71 eV in $CuGeO_3$ to 1.98 in $LiCu_2O_2$ and to 2.30 eV in Li_2CuO_2. In $LiVCuO_4$ there are two apical O ions as in $CuGeO_3$ but the apical bond lengths are much shorter as compared to $CuGeO_3$, 2.49 versus 2.76 Å (see Refs. 16 and 17). The d_{xy} to d_{z^2} excitation energy in $LiVCuO_4$ is thus substantially lower, 1.18 eV, even lower than in La_2CuO_4, where the apical bond length is 2.40 Å and the transition to the d_{z^2} orbital occurs at about 1.4 eV.[9,10] However, one additional effect which comes into play in $LiVCuO_4$ is the strong covalency between the V ions and both in-plane and apical O neighbors of the Cu sites. Such covalency effects on the VO_4 tetrahedra, see Fig. 2, give rise to large deviations from the formal V^{5+} and O^{2-} valence states employed in a fully ionic picture. When large deviations from the formal value of $2-$ occur for the effective charges of *all* adjacent O ions, the strongest affected is actually the ground-state energy because there are four O neighbors to which the lobes of the Cu d_{xy} orbital are directed. This "destabilization" of the ground-state energy of $LiVCuO_4$ explains the nearly uniform downward shift of the $d_{x^2-y^2}$, d_{yz}, and d_{xz} excited hole states, by about 0.15 eV as compared to $CuGeO_3$ (see Table III).

D. CuO

In spite of its apparent simple chemical formula cupric oxide, CuO, is a complex material. It was for instance only very recently discovered that it develops at the AF transition temperature T_N of 230 K also a net ferroelectric polarization, which is of substantial experimental[52] and theoretical[53,54] interest. As the ferroelectricity is completely due to magnetism, CuO is classified as a type-II multiferroic.[55] The complexity of this material system is related to the fact that each of the distorted CuO_6 octahedra shares corners and edges with fourteen other, adjacent octahedra. As for most of the Cu oxides, on a given octahedron the two apical-like Cu–O bonds are much longer than the other four Cu–O bonds, 2.78 versus 1.95 or 1.96 Å.[20] The quantum chemical calculations were therefore carried out on a cluster whose active region $\mathcal{C}_A$ is defined by one reference CuO_4 plaquette and the nearest fourteen Cu neighbors, see Fig. 3. The buffer region $\mathcal{C}_B$ includes the apical O ions of the reference Cu site and for each adjacent Cu ion the nearest four ligands.
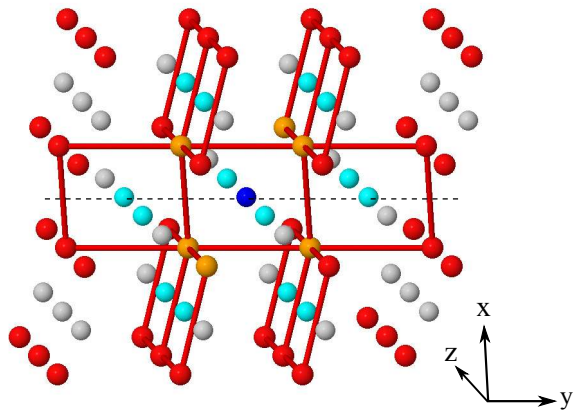

FIG. 3. Crystal structure of CuO and sketch of the cluster used for the calculations. The reference Cu and the fourteen adjacent Cu sites are shown in dark and light blue, respectively. O ions of the central octahedron are depicted in orange. The thin dashed line parallel to the y-axis connects the central Cu site and two Cu NN's along the same chain of edge-sharing CuO_4 plaquettes. For each apical O, there are two NN Cu ions on adjacent chains parallel to the y-axis.

TABLE IV. CASSCF and MRCI d–d excitation energies for CuO, see text. The MRCI values include Davidson corrections.[35] All numbers are in eV.

Hole orbital	CASSCF	MRCI-1	MRCI-2
xy	0	0	0
$x^2 - y^2$	1.13	1.37	1.38
yz	1.54	1.75	1.79
xz	1.60	1.81	1.85
z^2	1.71	1.93	1.96

CASSCF and MRCI results for the Cu d-level splittings in CuO are given in Table IV. CASSCF calculations were first performed for a FM configuration of the fifteen Cu d^9 sites. A non-standard local reference system was chosen for the central Cu site, with a rotation of 45° around z as for the cuprates discussed in Sec. III.C. The ground-state hole orbital is d_{xy} in this framework. CASSCF relative energies for the crystal-field excited states are listed in the second column of Table IV.

In a next step, MRCI calculations were carried out. Due to the large number of open-shell NN Cu sites, for CuO we were forced to restrict the CAS orbital reference space to the set of $3d$ orbitals of the central Cu ion. Two different types of approximations were employed. In a first set of restricted multiconfiguration calculations, out of the fourteen linear combinations of NN Cu d_{xy} functions, we froze the occupation of the seven lowest-energy (bonding-like) orbitals to 2 while the occupation of the higher-lying (antibonding-like) orbitals was restricted to 0. Only the Cu $3s$, $3p$, $3d$ and O $2p$ electrons on the central CuO$_4$ plaquette were correlated in the subsequent MRCI treatment. The difference between the CASSCF and MRCI values for each particular state in this set of CASSCF and MRCI calculations was added afterwards to the initial CASSCF d–d splitting. The resulting numbers are listed in the third column of Table IV. In the second set of MRCI calculations, we replaced the Cu^{2+} d^9 neighbors by closed-shell Zn^{2+} d^{10} ions. Those MRCI correlation induced corrections were again added to the initial CASSCF d–d excitation energies and the corresponding results are given in the fourth column of Table IV. As shown in Table IV, the MRCI treatment brings shifts of 0.2 to 0.25 eV to the CASSCF splittings. In the two approximation schemes, the MRCI corrections for each particular state are nearly the same, i.e., the MRCI correlation energies do not depend on details of the NN $3d$ electron configuration.

The lowest crystal-field excitation is from d_{xy} to $d_{x^2-y^2}$ and estimated in Table IV at about 1.4 eV. This value compares well with the measured optical gap, 1.3–1.6 eV.[56–59] RIXS measurements on CuO by Ghiringhelli et al.[60] show that most of the weight of the d–d excitation spectrum is between 1.7 and 2.3 eV, with clear peaks at 1.85 and 2.15 eV. Our MRCI data seem to somewhat underestimate those RIXS results, even when a $J \ln 2$ cor-

rection is considered to account for the superexchange interactions along the AF chains in CuO.[61] More flexible Cu and O basis sets are expected to further reduce these small differences between theory and experiment.

E. A ladder cuprate: CaCu$_2$O$_3$

In the so-called ladder compounds, the transition-metal ions are arranged in a planar network of ladders which can display two or more legs. These systems became subject of intense study when Dagotto et al.[62] found theoretical evidence that the isolated $S = 1/2$ AF two-leg ladder has a finite spin gap, i.e., a finite energy is needed to create a spin excitation.

Physical realizations are found in the vanadium oxide compound CaV$_2$O$_5$[63] and in cuprates such as CaCu$_2$O$_3$, SrCu$_2$O$_3$,[64] and (Sr,Ca)$_{14}$Cu$_{24}$O$_{41}$.[65] The latter compound also displays superconductivity.[66]

We analyze in this section the d-level electronic structure of CaCu$_2$O$_3$. For most of the two-leg ladder cuprates, including CaCu$_2$O$_3$, octahedra on the same ladder share common corners while adjacent octahedra on different ladders share common edges. One peculiar feature of CaCu$_2$O$_3$ is that on each rung of a ladder the Cu–O–Cu angle is 123°, much smaller than in other ladder compounds.[21] This is the reason the intersite magnetic couplings across the rungs are AF and small, about 10 meV, while the superexchange along the leg of the ladder is AF and one order of magnitude larger, about 135 meV.[67] In other words, from the magnetic point of view the system is rather 1D, with weakly interacting AF CuO$_2$ chains. Choosing the a-axis parallel to the rung and b along the leg of the ladder, the ground-state hole orbital is $d_{x^2-y^2}$.

The quantum chemical calculations were carried out on a cluster whose active region $\mathcal{C}_A$ is defined by one reference CuO$_4$ plaquette and the five adjacent Cu ions (one Cu NN on the same rung, two leg NN's, and two Cu NN's on an adjacent ladder). The buffer region $\mathcal{C}_B$ includes the two apical O ions of the reference Cu site, the nearest four ligands for each adjacent Cu ion, and six Ca neighbors. The apical O ligands are at rather large distance from the central Cu site, 3.0 Å.[21]

CASSCF and MRCI results for the Cu d-level splittings

TABLE V. CASSCF and MRCI d–d excitation energies for the ladder system CaCu$_2$O$_3$ (eV). The MRCI values include Davidson corrections.[35]

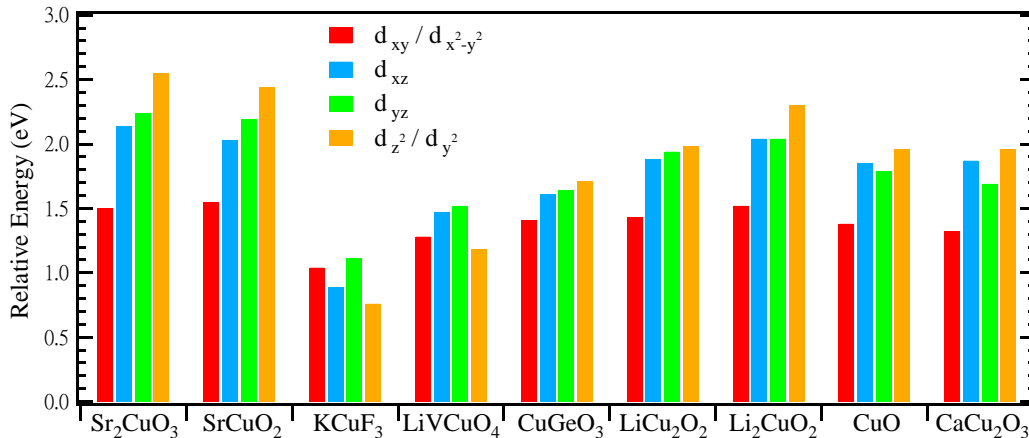| Hole orbital	CASSCF	MRCI
$x^2 - y^2$	0	0
xy	1.09	1.32
yz	1.46	1.69
xz	1.61	1.87
z^2	1.67	1.96

FIG. 4. MRCI Cu d–d excitation energies in 1D Cu d^9 compounds. Depending on the reference coordinate system, see text, the symmetry of the lowest t_{2g} hole state (in red) is denoted either as d_{xy} (corner-sharing chains of plaquettes or octahedra) or $d_{x^2-y^2}$ (edge-sharing chains). For KCuF$_3$, the e_g excited state (in orange) has y^2 symmetry. For all other compounds, the e_g excited state has z^2 symmetry.

in CaCu$_2$O$_3$ are listed in Table V. The MRCI treatment and the Davidson corrections bring shifts of 0.2 to 0.3 eV to the CASSCF d–d excitation energies. The excitation energies to the xz, yz, and z^2 orbitals are somewhat smaller than in Sr$_2$CuO$_3$, SrCuO$_2$, and Li$_2$CuO$_2$ because in the latter compounds there are no apical ligands. At the same time, the splitting between $d_{x^2-y^2}$ and d_{z^2} is larger than in the other cuprates investigated here, see Fig. 4, because the apical Cu–O bond length is the largest in CaCu$_2$O$_3$.

IV. CONCLUSIONS

It has been shown here that wavefunction-based electronic-structure calculations are well-suited for computing local charge excitations as observed in transition-metal oxides by optical and RIXS measurements. While this was demonstrated previously for a number of layered cuprates,[10] we have extended here those applications to 1D and ladder compounds. Results and trends for the d–d excitations in low-dimensional cuprates are summarized in Fig. 4. The *ab initio* data compare well with the results of optical absorption measurements on KCuF$_3$[43] and somewhat underestimate the excitation energies found by RIXS experiments for CuO.[60] Future RIXS experiments on other 1D cuprates included in Fig. 4 will constitute a direct test for the symmetry and energy of the different d–d excitations that we predict here.

From a more general perspective, the results reported here clearly indicate the significant potential of the *ab initio* wavefunction-based methods in the context of correlated electronic materials and the need to further develop such techniques in parallel with approaches based on density functional theory. The latter has revolutionized the field of electronic-structure calculations but its limits are also clear. Computations of excited states of strongly correlated electrons are in a way the worst case for DFT. One is then forced to avail oneself to alternatives, i.e., wavefunction-based methods. An attractive feature is that strong correlations can be handled by CASSCF calculations even when we deal with infinite periodic systems. In all approximations which are being made, the accuracy of the wavefunction-based methods can be progressively increased. Here we supplemented the CASSCF calculations by MRCI, yet, alternative supplementary methods are possible. Further exploration of such *ab initio* techniques is planned for the future.

[1] J. H. de Boer and J. W. Verwey, Proc. Phys. Soc. (London) **49**, 59 (1937); N. F. Mott and R. Peierls, Proc. Phys. Soc. (London) **49**, 72 (1937).

[2] H. Eskes and G. A. Sawatzky, Phys. Rev. B **44**, 9656 (1991).

[3] Y. Ohta, T. Tohyama, and S. Maekawa, Phys. Rev. B **43**, 2968 (1991).

[4] R. Raimondi, J. H. Jefferson, and L. F. Feiner, Phys. Rev. B **53**, 8774 (1996).

[5] L. Hozoi, M. S. Laad, and P. Fulde, Phys. Rev. B **78**, 165107 (2008).

[6] H. Sakakibara, H. Usui, K. Kuroki, R. Arita, and H. Aoki, Phys. Rev. Lett. **105**, 057003 (2010).

[7] R. Newman and R. M. Chrenko, Phys. Rev. **114**, 1507 (1959); G. W. Pratt, Jr. and R. Coelho, Phys. Rev. **116**, 281 (1959).

[8] L. J. P. Ament, M. van Veenendaal, T. P. Devereaux, J. P. Hill, and J. van den Brink, Rev. Mod. Phys. **83**, 705 (2011).

[9] M. Moretti Sala, V. Bisogni, L. Braicovich, C. Aruta, G. Balestrino, H. Berger, N. B. Brookes, G. M. De Luca, D. Di Castro, M. Grioni, M. Guarise, P. G. Medaglia, F. Miletto Granozio, M. Minola, M. Radovic, M. Salluzzo, T. Schmitt, K.-J. Zhou, and G. Ghiringhelli, New J. Phys. **13**, 043026 (2011).

[10] L. Hozoi, L. Siurakshina, P. Fulde, and J. van den Brink, Nature Sci. Rep. **1**, 65 (2011).

[11] C. de Graaf and R. Broer, Phys. Rev. B **62**, 702 (2000).

[12] CRYSTAL 2000, University of Torino, Italy.

[13] D. R. Lines, M. T. Weller, D. B. Currie, and D. M. Ogborne, Mater. Res. Bull. **26**, 323 (1991).

[14] M. Heinau, R. Baumann, B. Nick, M. Hartweg and L. Walz, Z. für Krist. 209, 418 (1994).

[15] R. H. Buttner, E. N. Maslen and N. Spadaccini, Acta Cryst. B, **46**, 131 (1990).

[16] M. Braden, G. Wilkendorf, J. Lorenzana, M. Ain, G. J. McIntyre, M. Behruzi, G. Heger, G. Dhalenne, and A. Revcolevschi, Phys. Rev. B **54**, 1105 (1996).

[17] M.A. Lafontaine, M. Leblanc, and G. Ferey, Acta Cryst. C **45**, 1205 (1989).

[18] F. Sapina, J. Rodriguez-Carvajal, M.J. Sanchis, R. Ibanez, A. Beltran, and D. Beltran, Solid State Commun. **74**, 779 (1990).

[19] W. Paszkowicz, M. Marczak, A. M. Vorotynov, K. A. Sablina, and G. A. Petrakovskii, Powder Diffr. **16**, 30 (2001).

[20] S. Asbrink and L. J. Norrby, Acta Crystallogr. B **26**, 8 (1970).

[21] V. Kiryukhin, Y.J. Kim, K.J. Thomas, F.C. Chou, R.W. Erwin, Q. Huang, M.A. Kastner, and R.J. Birgeneau, Phys. Rev. B **63**, 144418 (2001).

[22] MOLPRO 2006, Cardiff University, United Kingdom.

[23] A. Stoyanova, L. Hozoi, P. Fulde, and H. Stoll, Phys. Rev. B **83**, 205119 (2011); A. Stoyanova, L. Hozoi, P. Fulde, and H. Stoll, J. Chem. Phys. **131**, 044119 (2009); L. Hozoi, U. Birkenheuer, P. Fulde, A. Mitrushchenkov, and H. Stoll, Phys. Rev. B **76**, 085109 (2007).

[24] L. Hozoi and P. Fulde, in *Computational Methods for Large Systems: Electronic Structure Approaches for Biotechnology and Nanotechnology*, edited by J. R. Reimers (John Wiley & Sons, Hoboken, 2011), Chapter 6.

[25] CRYSTAL-MOLPRO interface, Max-Planck-Institut für Physik komplexer Systeme, Dresden, Germany.

[26] For a monograph, see T. Helgaker, P. Jørgensen, and J. Olsen, *Molecular Electronic-Structure Theory* (Wiley, Chichester, 2000).

[27] H. Suzuura, H. Yasuhara, A. Furusaki, N. Nagaosa, and Y. Tokura, Phys. Rev. Lett. **76**, 2579 (1996).

[28] N. Motoyama, H. Eisaki, and S. Uchida, Phys. Rev. Lett. **76**, 3212 (1996).

[29] J. Lorenzana and R. Eder, Phys. Rev. B **55**, 3358 (1997).

[30] C. de Graaf and F. Illas, Phys. Rev. B **63**, 014404 (2000).

[31] I. A. Zaliznyak, H. Woo, T. G. Perring, C. L. Broholm, C. D. Frost, and H. Takagi, Phys. Rev. Lett. **93**, 087202 (2004).

[32] H. Rosner, H. Eschrig, R. Hayn, S.-L. Drechsler and J. Málek, Phys. Rev. B **56**, 3402 (1997).

[33] C. Kim, Z. X. Shen, N. Motoyama, H. Eisaki, S. Uchida, T. Tohyama, and S. Maekawa, Phys. Rev. B **56**, 15589 (1997); H. Fujisawa, T. Yokoya, T. Takahashi, S. Miyasaka, M. Kibune, and H. Takagi, Phys. Rev. B **59**, 7358 (1999).

[34] B. J. Kim, H. Koh, E. Rotenberg, S.-J. Oh, H. Eisaki, N. Motoyama, S. Uchida, T. Tohyama, S. Maekawa, Z.-X. Shen, and C. Kim, Nature Phys. **2**, 397 (2006).

[35] The Davidson term corrects for the lack of quadruple and higher excitations in the MRCI expansion, see, e.g., Ref. 26.

[36] H. A. Bethe, Z. Phys. **71**, 205 (1931).

[37] J. des Cloizeaux and J. J. Pearson, Phys. Rev. **128**, 2131 (1962).

[38] L. D. Fadeev and L. A. Takhtajan, Phys. Lett. A **85**, 375 (1981).

[39] S. Kadota, I. Yamada, S. Yoneyama, and K. Hirakawa, J. Phys. Soc. Jpn. **23**, 751 (1967).

[40] K. I. Kugel and D. I. Khomskii, Usp. Fiz. Nauk. **136**, 621 (1982) [Sov. Phys. Usp. **25**, 231 (1982)].

[41] D. A. Tennant, S. E. Nagler, D. Welz, G. Shirane, and K. Yamada, Phys. Rev. B **52**, 13381 (1995).

[42] D. A. Tennant, T. G. Perring, R. A. Cowley, and S. E. Nagler, Phys. Rev. Lett. **70**, 4003 (1993).

[43] J. Deisenhofer, I. Leonov, M. V. Eremin, Ch. Kant, P. Ghigna, F. Mayr, V. V. Iglamov, V. I. Anisimov, and D. van der Marel, Phys. Rev. Lett. **101**, 157406 (2008).

[44] M. Enderle, B. Fåk, H.-J. Mikeska, R. K. Kremer, A. Prokofiev and W. Assmus, Phys. Rev. Lett. **104** 237207 (2010).

[45] S.-L. Drechsler, S. Nishimoto, R. O. Kuzian, J. Málek, W. E. A. Lorenz, J. Richter, J. van den Brink, M. Schmitt, and H. Rosner, Phys. Rev. Lett. **106**, 219701 (2011).

[46] S. Nishimoto, S.-L. Drechsler, R. O. Kuzian, J. van den Brink, J. Richter, W. E. A. Lorenz, Y. Skourski, R. Klingeler, and B. Büchner, Phys. Rev. Lett. **107**, 097201 (2011).

[47] M. Hase, I. Terasaki, and K. Uchinokura, Phys. Rev. Lett. **70**, 3651 (1993).

[48] K. Hirota, D. E. Cox, J. E. Lorenzo, G. Shirane, J. M. Tranquada, M. Hase, K. Uchinokura, H. Kojima, Y. Shibuya, and I. Tanaka, Phys. Rev. Lett. **73**, 736 (1994).

[49] T. Masuda, A. Zheludev, B. Roessli, A. Bush, M. Markina, and A. Vasiliev, Phys. Rev. B **72**, 014405 (2005).

[50] A. A. Gippius, E. N. Morozova, A. S. Moskvin, A. V. Zalessky, A. A. Bush, M. Baenitz, H. Rosner, and S.-L. Drechsler, Phys. Rev. B **70**, 020406 (2004).

[51] S.-L. Drechsler, J. Málek, J. Richter, A. S. Moskvin, A. A. Gippius, and H. Rosner, Phys. Rev. Lett. **94**, 039705 (2005).

[52] T. Kimura, Y. Sekio, H. Nakamura, T. Siegrist and A. P. Ramirez, Nature Mater. **7**, 291 (2008).

[53] M. Mostovoy, Nature Mater. **7**, 269 (2008).

[54] G. Giovannetti, S. Kumar, A. Stroppa, J. van den Brink, S. Picozzi, and J. Lorenzana, Phys. Rev. Lett. **106**, 026401 (2011).

[55] J. van den Brink and D. Khomskii, J. Phys.: Condens. Matter **20**, 434217 (2008).

[56] F. P. Kottyberg and F. A. Benko, J. Appl. Phys. **53**, 1173 (1982).

[57] J. Ghijsen, L. H. Tjeng , J. van Elp , H. Eskes, J. Westerink, G. A. Sawatzky and M. T. Czyzyk, Phys. Rev. B **38**, 11322 (1988).

[58] F. Marabelli, G. B. Parravicini, and F. Salghetti-Drioli, Phys. Rev. B **52**, 1433 (1995).

[59] T. Ito, H. Yamaguchi, T. Masumi and S. Adachi, J. Phys. Soc. Jpn. **67**, 3304 (1998).

[60] G. Ghiringhelli, A. Piazzalunga, X. Wang, A. Bendounan, H. Berger, F. Bottegoni, N. Christensen, C. Dallera, M. Grioni, J.-C. Grivel, M. Moretti Sala, L. Patthey, J. Schlappa, T. Schmitt, V. Strocov, and L. Braicovich, Eur. Phys. J. Special Topics **169**, 199 (2009).

[61] The NN AF J is approximately 70 meV in CuO, see Refs. 68 and 69.

[62] E. Dagotto, J. Riera, and D. Scalapino, Phys. Rev. B **45**, 5744 (1992); T. Barnes, E. Dagotto, J. Riera, and E. S. Swanson, Phys. Rev. B **47**, 3196 (1993).

[63] M. Onoda and N. Nishiguci, J. Solid State Chem. **127**, 359 (1996); H. Iwase, M. Isobe, Y. Ueda and H. Yasuoka, J. Phys. Soc. Jpn. **65**, 2397 (1996).

[64] M. Azuma, Z. Hiroi, M. Takano, K. Ishida, and Y. Kitaoka, Phys. Rev. Lett. **73**, 3463 (1994).

[65] E. M. McCarron, M. A. Subramanian, J. C. Calabrese and R. L. Harlow, Mater. Res. Bull. **23**, 1355 (1988); T. Siegrist, L. F. Schneemeyer, S. A. Sunshine, J. V. Waszczak and R. S. Roth, Mater. Res. Bull. **23**, 1429 (1988).

[66] M. Uehara, T. Nagata, J. Akimitsu, H. Takahashi, N. Mŏri, and K. Kinoshita, J. Phys. Soc. Jpn. **65**, 2764 (1996).

[67] E. Bordas, C. de Graaf, R. Caballol, and C. J. Calzado, Phys. Rev. B **71**, 045108 (2005).

[68] B. X. Yang, T. R. Thurston, J. M. Tranquada, and G. Shirane, Phys. Rev. B **39**, 4343 (1989).

[69] T. Shimizu, T. Matsumoto, A. Goto, K. Yoshimura, and K. Kosuge, J. Phys. Soc. Jpn. **72**, 2165 (2003).